SUPERCOIL, a Layout Model for Tokamaks with Superconducting TF Coils

K. Borrass, M. Söll

IPP 4/207 June 1982

MAX-PLANCK-INSTITUT FÜR PLASMAPHYSIK

8046 GARCHING BEI MÜNCHEN

MAX-PLANCK-INSTITUT FÜR PLASMAPHYSIK

GARCHING BEI MÜNCHEN

SUPERCOIL, a Layout Model for Tokamaks with Superconducting TF Coils

K. Borrass, M. Söll

IPP 4/207 June 1982

Die nachstehende Arbeit wurde im Rahmen des Vertrages zwischen dem Max-Planck-Institut für Plasmaphysik und der Europäischen Atomgemeinschaft über die Zusammenarbeit auf dem Gebiete der Plasmaphysik durchgeführt.

IPP 4/207

SUPERCOIL, a Layout Model for Tokamaks with Superconducting TF Coils

K. Borrass, M. Söll

June 1982

SUPERCOIL is a model for the self-consistent layout of ignited tokamaks with superconducting TF coils and a normal-conducting or superconducting OH transformer. The main components involved are the plasma, the TF system and the OH transformer. The model takes into account all physical, technical and geometrical constraints relevant to the basic layout of a tokamak. Among the solutions of the basic equations that meet all constraints the one optimized with respect to a prescribed figure of merit is determined. The paper contains the full set of model equations and a description of the solution method. The validity of the model is assessed by applying it to the present INTOR layout.

CONTENTS

1. Introduction

2. Description of Model

2.1 Geometry

2.2 Basic Equations
2.2.1 Geometric Relations
2.2.2 Plasma-related Quantities
2.2.3 Toroidal Field System
2.2.4 Computation of the Central Support Cylinder
2.2.5 Normal-conducting OH Transformer
2.2.6 Superconducting OH Transformer
2.2.7 Figure of Merit

2.3 Constraints and Optimization

3. Illustrative Example

1. INTRODUCTION

SUPERCOIL is a model for the self-consistent layout of ignited tokamaks with superconducting TF coils and a normal-conducting or superconducting OH transformer. It was developed from the NORMCOIL layout model for normal-conducting tokamaks, and hence the underlying philosophy is the same.[1] This philosophy is based on the observation that in practice the layout of a tokamak is largely determined by performance objectives and the specific design characteristics of the particular system. Typical performance objectives of an ignited tokamak are, for instance, its ignition margin, the minimum wall load or the minimum neutron fluence. Typical design options are the heating or maintenance concept. Formally such objectives or specifications enter as constraints that have to be met when solving the underlying model equations. In SUPERCOIL, in a certain sense, only such constraints enter as input. Quantities such as the plasma radius, the magnetic field at the coils, etc. are only prescribed if desired. Of the solutions of the model that meet all constraints the one that minimizes or maximizes a prescribed figure of merit is selected. A specific feature of the solution method used in SUPERCOIL is that the basic model equations are always solved in the same order, irrespective of the constraints and figure of merit under consideration. Maximum flexibility is thus achieved as to the implementation of different constraints and figures of merit.

The main components involved in SUPERCOIL are the plasma, the TF coil system and the OH transformer. The interaction of these components governs the basic layout features of a tokamak. For the OH trans-

former both a normal-conducting and a superconducting option are provided.

The general arrangement of the main components is described in Sec. 2.1. The next section presents the basic model equations. The solution method is described in Sec. 2.3 in greater detail. This section also contains a description of the constraints that are taken into account. The validity of the model is checked in Sec. 2.4 by applying it to the present INTOR layout point.

2. DESCRIPTION OF MODEL

2.1 Geometry

The anlysis is based on tape-wound D-coil systems as shown in Fig. 1. The plasma is centred at R_o (plasma major radius). The elongated plasma cross-section is characterized by the minor radius a and the plasma elongation s. The plasma is surrounded by a scrape-off layer of thickness ℓ, a vessel of thickness u and a shielding of thickness D. A blanket of thickness DB_1 and DB_2 is provided at the inner and outer sides respectively.

The D-coil is characterized by the minimum and maximum distances of the centre line from the torus axis, R_1 and R_2 respectively, and by the coil thickness Δ. δ is the sum of the thermal insulation and coil casing thickness.

The coils are tapered in the inner coil region in order to make optimum use of the limited area in this region. A common cryostat is assumed for the whole TF system.

The toroidal field coils are supported by the central support cylinder of thickness t_1 (see Fig. 2). The ohmic heating coil has a thickness Δt and a radius R_{OH} as shown in Fig. 2.

There are further important geometrical parameters, namely g, ΔR and d, of which g and ΔR are visualized in Fig. 1. The parameter g characterizes the horizontal bore available for the installation of, for instance, a poloidal divertor. ΔR characterizes the horizontal bore. The parameter d^* is the bore between two coils in the equatorial plane (see Fig. 3). $d=d^*-2\,D$ gives the free space available for beam ducts etc. Depending on the specific system under consideration, lower limits g^m, ΔR^m and d^m exist for the quantities g, ΔR and d.

2.2 Basic Equations

The following set of equations forms the central part of the model. They can be evaluated in the given order, once the first two groups of parameters of Table I are given. The relations are only commented on if necessary. All units are mksa units if not otherwise stated.

2.2.1 Geometric Relations

$$a^* = a\sqrt{s} \tag{1}$$

(radius of an equivalent circular plasma)

$$R_o = a\,A \tag{2}$$

(plasma major radius)

$$V = 2\pi^2\, a^{*2}\, R_o \tag{3}$$

(plasma volume)

$$R_1 = R_o - a - \ell - D - u - DB_1 - \delta - \Delta/2 \qquad (4)$$

(see Fig. 1)

$$d^* = \frac{2\,\pi(R_o + a + \ell + u)}{N\ I_d} + \frac{d_1}{I_d} + d_2 \qquad (5)$$

d^* is the miminum horizontal distance (in the equatorial plane) between two TF coils, such that a module of an N times I_d (I_d = 1, 2, ...) segmented blanket can be moved radially outward (maintenance conditions, see Fig. 3). The constants d_1 and d_2 can be used to take into account off-horizontal plane effects. They have to be calibrated according to the specific situation. Typically the second and third terms in eq. (5) are minor corrections.

$$d_o^* = \max\left\{ d^*,\ d^m + 2\,D \right\} \qquad (6)$$

d_o^* is the minimum distance between two coils such that the maintenance condition and the condition $d \geq d^m$ are fulfilled. Note that the shielding in the space between two coils is also assumed to be of thickness D.

$$h_o = s\ a + \ell + D + u + DB_2 + g^m \qquad (7)$$

h_o is the minimum value of the coil height h such that $g \geq g^m$ holds (see Fig. 1).

$$R_{20} = R_o + a + \ell + u + D + DB_2 + \delta + \Delta R^m + \Delta/2 \qquad (8)$$

R_{20} is the minimum value of R_2 such that $\Delta R \geq \Delta R^m$ holds.

$$R'_{20} = R_1 + \Delta + \delta + \frac{(d_o^* + 2\delta)\,N}{2\,\pi} \qquad (9)$$

R'_{20} is the minimum value of R_2 such that the maintenance condition and the condition $d \geq d^m$ are fulfilled.

$$R''_{20} = R_1 \left(\left(125.686 + (h_o + \delta + \Delta/2)\ 29.907/R_1 \right)^{0.5} - 10.1038 \right) \qquad (10)$$

R''_{20} is the minimum value of R_2 such that $g \geq g^m$ holds. See also eq. (13).

$$R'_2 = \max \left\{ R_{20},\ R'_{20},\ R''_{20} \right\} \qquad (11)$$

R'_2 is the minimum value of R_2 such that the constraints $g \geq g^m$, $\Delta R \geq \Delta R^m$, $d \geq d^m$ and the maintenance conditions are met.

$$R_2 = R'_2 + Y \qquad (12)$$

Y is an auxiliary quantity which is always positive. Its role is explained in Sec. 2.3.

$$h = R_1 \left(3.3437 \times 10^{-2} \left(R_2/R_1 \right)^2 + 6.7568 \times 10^{-1}\ R_2/R_1 - 0.78911 \right) - \Delta/2 - \delta \qquad (13)$$

This is a polynominal fit of an analytical expression given in Ref. 8. The inverse relation was used in eq. (10).

$$g = h - s\ a - \ell - u - DB_2 - D \qquad (14)$$

(see Fig. 1)

$$d = \frac{2\pi (R_2 - R_1 - \delta - \Delta)}{N} - 2\ D - 2\ \delta \qquad (15)$$

(horizontal bore for beam ducts etc.)

$$\Delta R = R_2 - R_{20} + \Delta R^m \qquad (16)$$

(see Fig. 1)

Equations (14), (15) and (16) give the actual values of the quantities g, d and ΔR respectively.

$$R = R_o + a \tag{17}$$

$$\varepsilon[\%] = 5.4\times10^{2}\ \frac{R\ R_1(R_2/R_1 - 1)^{1.5}(R_2 - R_1\eta_2)}{N^4((R_2-R)^2 + (\pi R_2/2N)^2)^{1.5}}$$

$$\frac{\pi^3 + 4\pi\ N^2(1-R/R_2)R/R_2}{\pi^2 + 4\ N^2(1-R/R_2)^2} \tag{18}$$

ε is the field ripple at point R.[3] The ripple definition used is $\varepsilon = 200\ (B_{max} - B_{min})/(B_{max} + B_{min})$. For definition of η_2 see eq. (34).

2.2.2 Plasma-related Quantities

$$\bar{\beta}_t = 0.12\ s/A \tag{19}$$

$\bar{\beta}_t$ is the volume-averaged toroidal beta (useful part). This scaling of $\bar{\beta}_t$ is widely accepted for not too strong elongation ($s < 2.0$) and not too low aspect ratios ($A > 2.5$).

$$B_t^o = \left(\frac{C}{\bar{\beta}_t^2\ a^{*\,2}}\right)^{1/4} \tag{20}$$

Equation (20) is the ignition condition for a plasma which is dominated by anomalous electron heat conduction of the ALCATOR type. ALCATOR type losses typically dominate neoclassical ion heat conduction, except for rather high densities. Bremsstrahlung losses can typically be neglected, provided that the working point is not located too far into the ignition regime (transport-dominated system). In this approximation the ignition condition simplifies to $Q_\alpha - Q_{loss} \geq 0$, where Q_α is the α-heating term and Q_{loss} the transport loss term in the energy balance.

With $Q_\alpha \sim \bar{\beta}_t^2 B_t^{o\,4} f(T)$ and $Q_{loss} \sim T/a^{*2}$ it then follows that ignition requires that $\bar{\beta}_t^2 B_t^{o\,4} a^{*2} \geq C$, where C can be taken as constant, if one assumes that the working temperature is close to the minimum of T/f(T). The constant C measures the safety of ignition, a value of $C \simeq 1.8$ corresponding to marginal ignition. Other transport models can easily be implemented. Confinement to ALCATOR scaling is useful to allow comparison with systems such as FED and INTOR, which have been studied in detail on the basis of this model.

$$p_f\ [MW\ m^{-3}] = 2.0\ \bar{\beta}_t^2\ B_t^{o4} \tag{21}$$

Using this approximation for the fusion power density p_f, it is assumed that T lies in the range where $\langle\sigma v\rangle \sim T^2$ is valid for the D-T reaction parameter. This is typically compatible with the assumption for T in the derivation of eq. (20). The factor of proportionality in eq. (21) depends on both the T and n profiles. The value of 2.0 can be achieved by moderately peaked T and nearly flat n-profiles. Even higher values could be obtained if the n-profiles were more peaked in large tokamaks than predicted by current transport codes.

$$P_f\ [MW] = V\ p_f \tag{22}$$

(fusion power)

$$P_\alpha\ [MW] = 0.2\ P_f \tag{23}$$

(α-power)

$$N_n\ [MW\ m^{-2}] = 0.4\ p_f\ \frac{a^{*2}}{a^*\,(1+s)/(2\,s^{1/2}) + \ell} \tag{24}$$

(mean neutron wall load)

$$W_{int}\ [MW\ y\ m^{-2}] = \frac{N_n\ \tau_{tot}}{3.154 \times 10^7} \qquad (25)$$

(integral wall load)

This equation is used to determine W_{int} if τ_{tot} is explicitely prescribed as an input parameter. Otherwise τ_{tot} is determined by the relation

$$\tau_{tot} = 3.154 \times 10^7\ W_{int}/N_n. \qquad (26)$$

$$\varphi_n = 4.427 \times 10^{17}\ \tau_{tot}\ N_n\ e^{-14.00\ D} \qquad (27)$$

(neutron dose behind the shielding)

$$T_c\ [g] = 1.779 \times 10^{-6}\ P_f\ \tau_{tot} \qquad (28)$$

(total tritium consumption)

$$I_p = \frac{2\pi B_t^o\ a^{*2}}{\mu_o q(a)\ R_o}\ \frac{1 + s^2}{2\ s} \qquad (29)$$

(plasma current)

$$\ell_i = 1 \qquad (30)$$

(internal plasma inductance per unit length in units of $\mu_o\ R_o/2$)

$$L_p = \mu_o\ R_o\ (\ell n\ (8\ R_o/a^*) - 2 + \ell_i/2) \qquad (31)$$

(plasma inductance)

$$V_s = f\ L_p\ I_p \qquad (32)$$

V_s is the total required OH flux swing. Resistive losses are estimated by taking $f > 1$.

2.2.3 Toroidal Field System

The calculation model of the TF coil system is based on the theory of "real D" coil systems - including the segmentation of the toroidal coil system - and on the stability and discharge criteria of cryogenically stabilized superconducting magnets.[4, 5] The principles of the TF calculation model are described in Ref. 6.

The radius of curvature ρ_2 at $R = R_2$ of the coil centre line is determined by the equation

$$R_1/R_2 = 1 - (1.984 + 4.336/N)\,(\rho_2/R_2) + (1.897 + 8.864/N)\,(\rho_2/R_2)^2 - (1.048 + 7.392/N)\,(\rho_2/R_2)^3 + (0.271 + 2.416/N)\,(\rho_2/R_2)^4. \quad (33)$$

In practice eq. (33) is solved by iteration.

$$\eta_2 = (2\pi R_1 - NB)/2\pi R_1 \quad (34)$$

(filling factor including the casing thickness B)

$$K = \frac{\rho_2}{R_2}\left(1 + \frac{1}{N}\right) + \frac{1}{N}\,\ell n \frac{2.27\,R_2}{\sqrt{\eta_2 2\pi R_1 \Delta N}} \quad (35)$$

(coil parameter)

For "ideal D" coil systems the parameter K is given by the formula[7]

$$K = \frac{1}{2}\,\ell n\left(\frac{R_2}{R_1}\right). \quad (36)$$

Equation (36) can be taken as an approximation for eq. (35), when

the equations of this section are used for calculations "by hand" and a solution of eq. (33) is not readily available.

$$F = 4\pi^2 K e^K \left[K I_o(K) + (K-1) I_1(K)\right] R_1 \left(R_1+\Delta/2\right)^2 \qquad (37)$$

("specific magnet volume" [8]). I_o and I_1 are modified Bessel functions of zero and first order respectively.

$$\bar{\varphi}_n[m^{-2}] = \frac{\varphi_n}{6\Delta}\left(1-e^{-6\Delta}\right) \qquad (38)$$

(average neutron dose)

φ_n is the neutron dose behind the shielding according to eq. (27).

$$B_m = \frac{B_t^o R_o}{R_1+\Delta/2} \qquad (39)$$

(maximum magnetic field at the inner winding edge $R_1 + \Delta/2$)

$$\rho_e^{Cu} = (2 + 0.18\, B_m)\, 10^{-10} + 4.4 \times 10^{-9} \left[1 - \exp\left(-2.8 \times 10^{-23} \bar{\varphi}_n\right)\right] \qquad (40)$$

$$\rho_e^{Al} = 10^{-10} + 9.4 \times 10^{-9} \left[1 - \exp\left(-2.8 \times 10^{-23}\, \bar{\varphi}_n\right)\right] \qquad (41)$$

ρ_e^{Cu} and ρ_e^{Al} are the specific resistivities of copper and aluminium, respectively, at liquid He temperatures. For copper a mean value for the magneto-resistivity (averaged over the total coil volume) is included by the term $0.18 \times 10^{-10}\, B_m$. The magneto-resistivity of aluminium does not follow the Kohler rule.[9] The influence of the magnetic field on ρ_e^{Al} is taken into account by a constant value. The increase of resistivity due to neutron irradiation is given by the last terms of eqs. (40) and (41). The use of copper or aluminium as stabilizer is optional in the code.

$$c_o^{Cu}\ [A^2\ s\ /\ m^4] = 5 \times 10^6/\rho_e^{Cu} + 5 \times 10^{15} \qquad (42)$$

("material function" for copper)

$$c_o^{Al}\ [A^2\ s\ /\ m^4] = 1.66 \times 10^6/\rho_e^{Al} + 2.44 \times 10^{15} \qquad (43)$$

("material function" for aluminium)

c_o^{Cu} and c_o^{Al} follow from safety discharge analysis.[5] A maximum temperature of the conductor of 50 K after a safety discharge is anticipated in eqs. (42) and (43).

$$A\ [m^2\ s^{0.8}/kg^{0.6}] = \left(\frac{F\ \rho_e^2}{8\pi \times 10^{-7}\ c_o V_m \dot{q}^2 h^2 \gamma^2}\right)^{0.2} \qquad (44)$$

(" stability parameter").

γ is the wetting parameter (fraction of the conductor surface which is in direct contact with the coolant). The parameter h is defined by $h = P_c / A_{st}$, where P_c and A_{st} are the perimeter of the conductor and the cross-sectional area of the stabilizer. In the program h and γ are combined to a single input parameter $H_g = \gamma h$.

$$j_c^I = \frac{0.66 \times 10^{10}\ [1-(T/9)^2]^{1.5}}{\sqrt{B_m}}\ \left[1 - \frac{B_m}{21\ [1-(T/9)^2]}\right] \qquad (45)$$

(critical current density for NbTi)

$$j_c^{II} = \frac{4 \times 10^{10}\ [1-(T/18)^2]^2}{[0.2\ (1-T/18)^2 + 1]^2 \sqrt{B_m}}\ \left[1 - \frac{B_m}{36[1-(T/18)^2]}\right]^2 \qquad (46)$$

(critical current density for Nb_3Sn)

$j_c^{I/II}$ is the critical current density at the coil centre, where a magnetic field value of $B = \frac{2}{3} B_m$ is taken. The value of $\frac{2}{3} B_m$ follows from our assumption that the winding is subdivided into three parts; each section is designed with its own conductor adapted to the corresponding magnetic field values. The conductor for the inner section is designed for $B = B_m$, that for the central section for $B = \frac{2}{3} B_m$ and that for the outer section for $B = \frac{1}{3} B_m$. The choice of NbTi and Nb_3Sn is optional to the code.

$$\sigma = \frac{10^7 \, K \, C_F \, (R_1 + \Delta/2)^2 \, B_m^2}{8\pi \, \eta_1 \, \eta_2 \, R_1 \, \Delta} \tag{47}$$

σ is the mechanical tensile stress for D-coils. C_F takes into account local stress enhancement caused, for instance, by the support structure etc. From finite element calculations a value of $C_F = 1.3$ seems to be adequate. [6] η_1 is the filling factor including the cooling ducts and electrical insulation in the coil winding.

$$E_m = 3.978 \times 10^5 \, F \, B_m^2 \tag{48}$$

(stored magnetic energy)

$$j_m^I = \frac{0.58 \times 10^{10} \, [1 - (T/9)^2] \, 1.5}{\sqrt{B_m + \Delta B_\perp}} \left[1 - \frac{(B_m + \Delta B_\perp)}{14[1-(T/9)^2]}\right] \tag{49}$$

$$j_m^{II} = \frac{2.2 \times 10^{10} \, [1-(T/18)^2]^2}{[0.2 \, (1-T/18)^2 + 1]^2 \sqrt{(B_m + \Delta B_\perp)}} \left[1 - \frac{(B_m + \Delta B_\perp)}{24[1-(T/18)^2]}\right]^2 \tag{50}$$

j_m^I and j_m^{II} are the minimum critical current densities at the inner coil edge ($R = R_1 + \Delta/2$) in the case of NbTi and Nb_3Sn respectively. The conductor is exposed there to the maximum toroidal field B_m and a field $\Delta B_\perp$ produced by the poloidal field coils. With eqs. (49) and (50)

auxiliary quantities are introduced to avoid violating superconducting critical parameter values (see Sec. 2.3).

$$\alpha = j_c \, B_m^{0.4} \, A \tag{51}$$

α is the average ratio of the cross-sectional area between stabilizer and superconductor.

$$\beta = \frac{4 \times 10^{-7} \, \pi \, \eta_1 \, \eta_2 \, R_1 \, \Delta \, j_c}{B_m \, (R_1 + \Delta/2)} - \alpha - 1 \tag{52}$$

β is the average ratio of the cross-sectional area between reinforcing material and superconductor.

$$\varepsilon = \frac{(R_1 + \Delta/2) \quad j_c \quad K \quad B_m}{2(E_{sc} + \alpha E_{st} + \beta E_r)} \tag{53}$$

(strain on the coil winding)

Equation (53) relates the strain on the coil winding (composite conductor: superconductor, stabilizer, reinforcing material) to the Young's moduli E_{sc} (superconductor), E_{st} (stabilizer) and E_r (reinforcing material).

The preceding equations describe the following layout procedures for a TF coil. First the amount of stabilizer is calculated. Then the amount of reinforcing material is determined under the condition that the total winding area not covered with stabilizing material is filled with reinforcing material. Then the strain value is calculated with eq. (53), and the value obtained is compared with the maximum allowable value. A solution is found if the calculated strain value is smaller than the maximum allowable strain, as will be discussed in Sec. 2.3.

$$j_{st} = j_c/\alpha \tag{54}$$

(current density averaged over the stabilizer cross-sectional area)

$$j_w = j_c \eta_1/(1 + \alpha + \beta) \tag{55}$$

(average current density in the coil winding)

$$I_o = (C_o V_m/E_m)^{-0.6} (\dot{q}\ h\gamma/\rho_e)^{0.8} \tag{56}$$

(optimum conductor current)

$$V_w = 4\ \pi^2 \eta_1 \eta_2\ R_1^2\ K\ e^K \Delta[I_o(K) + I_1(K)] \tag{57}$$

(total volume of the winding material)

$$V_{sc} = V_w/(1 + \alpha + \beta) \tag{58}$$

(total volume of the superconductor)

$$M_{sc} = \rho_{sc}\ V_{sc} \tag{59}$$

(total mass of the superconductor)

$$V_{st} = \alpha V_{sc} \tag{60}$$

(total volume of the stabilizer)

$$M_{st} = \rho_{st}\ V_{st} \tag{61}$$

(total mass of the stabilizer)

$$V_r = \beta\ V_{sc} \tag{62}$$

(total volume of the reinforcing material)

$$M_r = \rho_r\ V_r \tag{63}$$

(total mass of the reinforcing material)

$$V_{ca} = 4\pi\, Ke^{K} R_1 B\, (2\pi \ell_{22} R_1 + N\Delta)\, (I_o + I_1) \tag{64}$$

(volume of the coil casing)

$$M_{ca} = \rho_{ca}\, V_{ca} \tag{65}$$

(mass of the coil casing)

$$\hat{a} = [I_o(1+\alpha)/j_c]^{0.5} \tag{66}$$

($\hat{a}$ is the effective conductor width, assuming a conductor with square cross-section)

$$W_h = V_{sc}\, \frac{4}{3\pi}\, J_o\, B_o\, d_f\, \ell n\, \left(\frac{B_o + B_m/2}{B_o}\right) \tag{67}$$

(hysteresis losses for coil excitation). J_o and B_o are constants and d_f is the diameter of a superconducting filament. For NbTi and a cooling temperature of T~4K the values J_o and B_o are about 10^{10} A/m^2 and 1 T respectively.

$$P^{\perp}_{e,c} = V_{st} \frac{\dot{B}^2_{\perp}\, \hat{a}^2}{12\, \rho_e} \tag{68}$$

$P^{\perp}_{e,c}$ are the eddy current losses of the conductor produced by a change of the magnetic field component directed perpendicular to the conductor axis at a rate $\dot{B}_{\perp}$.

$$P^{''}_{e,c} = V_{st} \frac{\dot{B}^2_{''}\, \hat{a}^2}{8\pi\, \rho_e} \tag{69}$$

$P^{''}_{e,c}$ are the eddy current losses of the conductor produced by a change of the parallel magnetic field component at a rate $\dot{B}_{''}$.

$$P_c^{\perp} = 2\, V_{sc}\, \dot{B}_{\perp}^2 \left(\frac{\ell_p}{2\pi}\right)^2 \left[0.5 + \ell n \sqrt{\frac{\pi(\alpha+1)}{8}}\right]/\rho_e \qquad (70)$$

(coupling losses produced by $B_{\perp}$)

Equation (70) was obtained on the assumption that the volume of the conductor core (superconducting filaments plus small amount of stabilizer) is twice the volume of the superconductor. ℓ_p is the twist length of the superconducting filaments.

$$P_c'' = 2\pi^2\, V_{sc}\, \frac{\dot{B}_{\shortparallel}^2\, \hat{a}^2}{3\rho_e} \qquad (71)$$

(coupling losses produced by $\dot{B}_{\shortparallel}$)

The above treatment of the conductor a.c. losses is based on Ref. 10.

$$L_o = 2\pi\, R_1\, K\, e^K\, [I_o(K) + I_1(K)] \qquad (72)$$

(circumference of a toroidal D-coil[8])

$$d_{ca} = (2\pi\, R_1\, \Delta/N)^{0.5} \qquad (73)$$

(effective width of the coil casing)

$$S_w = \eta_2\, 2\pi R_1\, \Delta/N \qquad (74)$$

(cross-sectional area of the winding)

$$L_{ca} = 2\,(\Delta + 2\pi R_1/N) \qquad (75)$$

(circumference of the coil casing)

$$P_{e,ca}^{\perp} = B\, d_{ca}^3\, \dot{B}_{\perp}^2\, L_o\, N/(6\, \rho_{e,ca}) \qquad (76)$$

$$P_{e,ca}'' = B\, S_w^2\, \dot{B}_{\shortparallel}^2 L_o N/(L_{ca}\, \rho_{e,ca}) \qquad (77)$$

Equations (76) and (77) give the eddy current losses in the coil casing, $\rho_{e,ca}$ is the specific resistivity of the casing material.

2.2.4 Central Support Cylinder

$$R_{cy}^{m,nc} = R_1 - \Delta/2 - \delta/2 \qquad (78)$$

$$R_{cy}^{m,sc} = R_1 - \Delta/2 \qquad (79)$$

$R_{cy}^{m,nc}$ and $R_{cy}^{m,sc}$ are the maximum radii of the central support cylinder in the case of a normal-conducting and superconducting OH transformer respectively. In eq. (78) we have assumed that half of the thermal insulation is inside and half outside the central support cylinder, and that the central support cylinder is cooled down to liquid N_2 temperature. In the superconducting case a common cryostat is assumed for TF coils and OH transformer.

The thickness t_1 of the central support cylinder is determined from the "collapsing criterium" of cylinders, which relates the maximum allowable external pressure to the maximum allowable stress σ_{cy}^m. (11)

$$\frac{B_m^2 \times 10^7}{8\pi} = \frac{\sigma_{cy}^m}{1+4\,\frac{\sigma_{cy}^m (R_{cy}^m - t_1/2)^2}{E_{cy}\, t_1^2}} \; \frac{t_1}{(R_{cy}^m - t_1/2)}. \qquad (80)$$

Equation (80) is solved iteratively to determine t_1. Unlike other constraints, eq. (80) always assigns to t_1 the smallest value compatible with the stress limit. This can be done without loss of generality since obviously for any reasonable figure of merit a support cylinder which is thicker than necessary is less favourable (internal optimization).

$$V_{cy} = 4\pi^2 (R_{cy}^m - t_1/2)\, t_1\, R_1\, K\, e^K\, I_1(K) \qquad (81)$$

$$N_{cy} = \rho_{cy} V_{cy} \tag{82}$$

(mass of the support cylinder)

2.2.5 Normal-conducting OH Transformer

To take into account the core constraint, the coupling of the OH coil to the plasma ring has to be considered. Figure 2 shows the OH coil arrangement and the notations used.

$$R_{OH}^{m} = R_1 - \Delta/2 - t_1 - \delta \tag{83}$$

(maximum OH coil radius)

$$\Delta t = X R_{OH}^{m} \tag{84}$$

is the thickness of the OH coil. X is an auxiliary quantity which is self-consistently determined with respect to the OH transformer constraints (see Sec. 2.3).

$$R_{OH} = R_{OH}^{m} - 0.5\ \Delta t \tag{85}$$

(OH coil radius)

$$B_{OH} = \frac{f\ I_p\ L_p}{\lambda \pi\ R_{OH}^2} \tag{86}$$

B_{OH} is the field at the OH coil. Equation (86) is the approximate transformer equation for the OH coil-plasma ring system. Equation (86) is pessimistic in that contributions by the vertical field are ignored.

To reduce the resistive losses in a normal-conducting OH coil, it may be appropriate to design the system so that a reduction of B_{OH} from its maximum value to a value close to zero already yields the required flux. Since typically most of the OH flux is consumed during start-up, B_{OH} and hence the losses can thus be kept at a low value during most of the burn phase.This can be taken into account by giving λ in eq. (86) a value close to unity. The typical case where the B_{OH} swing is twice its maximum value is given by $\lambda = 2$.

$$j_{OH} = \frac{B_{OH}}{\mu_o \, \Delta t} \tag{87}$$

(OH current density)

$$\sigma_{OH} = B_{OH}^2 \frac{(R_{OH}^2 + \Delta t^2/4)}{2 \, \mu_o \, \Delta t \, R_{OH}} \tag{88}$$

(OH coil tensile stress)

The core constraint is established by imposing limits on j_{OH} and σ_{OH} (see Sec. 2.3).

2.2.6 Superconducting OH Transformer

$$R_{OH}^m = R_1 - \Delta/2 - t_1 \tag{89}$$

(maximum OH coil radius)

Neglecting the thermal insulation thickness on the right-hand side of eq. (89), we implicitly assume a common cryostat for TF coils and OH transformer.

$$\Delta t = X \, R_{OH}^m \tag{90}$$

is the thickness of the OH coil. As to the quantity X the same remark applies as in the normal-conducting case.

$$R_{OH} = R^{m}_{OH} - 0.5\,\Delta t \tag{91}$$

(OH coil radius)

$$B_{OH} = \frac{f\, I_p\, L_p}{2\pi\, R^2_{OH}} \tag{92}$$

(field at the OH coil)

$$\rho^{Cu}_{e,OH} = (2.0 + 0.18\, B_{OH})\, 10^{-10} \tag{93}$$

$$\rho^{Al}_{e,OH} = 10^{-10} \tag{94}$$

$\rho^{Cu}_{e,OH}$ and $\rho^{Al}_{e,OH}$ are the specific resistivities of copper and aluminium respectively. Unlike in the resistivity formulas used in Sec. 2.2.3, the influence of the neutron radiation is ignored.

$$j^{I}_{c,OH} = \frac{0.66 \times 10^{10}\, (1-(T/9)^2)^{1.5}}{B^{1/2}_{OH}} \left(1-\frac{B_{OH}}{21\,(1-(T/9)^2)}\right) \tag{95}$$

$$j^{II}_{c,OH} = \frac{4 \times 10^{10}\, (1-(T/18)^2)^2}{(0.2\,(1-T/18)^2 + 1)^2\, B^{1/2}_{OH}} \cdot \left(1-\frac{B_{OH}}{36\,(1-(T/18)^2)}\right)^2 \tag{96}$$

(critical OH transformer current density for NbTi and Nb_3Sn respectively)

$$j^{I}_{m,OH} = \frac{0.58 \times 10^{10}\, (1-(T/9)^2)^{1.5}}{B^{1/2}_{OH}} \cdot \left(1-\frac{B_{OH}}{14\,(1-(T/9)^2}\right) \tag{97}$$

(minimum critical current density in a NbTi OH transformer).

$$j^{II}_{m,OH} = 2.2 \times 10^{10}\, \frac{(1-(T/18)^2)^2}{(0.2\,(1-T/18)^2 + 1)^2\, B^{1/2}_{OH}} \cdot \left(1-\frac{B_{OH}}{24(1-(T/18)^2)}\right)^2 \tag{98}$$

(minimum critical current density in a Nb_3Sn OH transformer).

$$A_{OH} = \rho_{e,OH}^2 \; / \; (\dot{q}\; h\; \gamma)^2 \qquad (99)$$

(stability parameter).

The difference between A_{OH} and the stability parameter according to eq. (44) is due to the restriction to cryogenically stabilized conductors for the OH transformer. In this case the conductor current I_{OH} has to be given as an input parameter instead of its following self-consistently from the safety discharge criterion.

$$\alpha_{OH} = j_{c,OH}\; (I_{OH}\; A_{OH})^{1/3} \qquad (100)$$

α_{OH} is the average ratio of the cross-sectional area between stabilizer and superconductor.

$$\beta_{OH} = 4\pi\; 10^{-7}\; j_{c,OH}\; \Delta t / B_{OH} - \alpha_{OH} - 1 \qquad (101)$$

β_{OH} is the average ratio of the cross-sectional area between reinforcing material and superconductor.

$$\varepsilon_{w,OH} = \frac{(R_{OH} - \Delta t/2)^2\; (R_{OH}^2 + \Delta t^2/4)\; B_{OH}^2}{2\mu_o \Delta t\; R_{OH}^3\; (E_{sc} + \alpha_{OH}\; E_{st} + \beta_{OH}\; E_r)}\; (1 + \alpha_{OH} + \beta_{OH}) \qquad (102)$$

(strain in the OH coil winding).

Equation (102) is analogous to eq. (53) but applies to a cylindrical coil.

2.2.7 Figure of Merit

A rough cost estimate is used as a figure of merit for the optimization procedure described below.

$$\phi_1\ [DM] = C_{mag}\ E_m \times 10^{-6} \qquad (103)$$

(investment costs).

Equation (103) estimates the investment costs in terms of the stored energy of the TF system.

$$\phi_2\ [DM] = C_{trit}\ T_c\ (1-R) \qquad (104)$$

(cost of the externally supplied tritium)

$$\phi_3\ [DM] = 3.171 \times 10^{-8}\ 0.05\ \tau_{tot}\ \phi_1/\xi \qquad (105)$$

ϕ_3 is an estimate of the cost for maintenance and repair, assuming 5 % of the investment cost for maintenance and repair per year.

$$\phi = \phi_1 + \phi_2 + \phi_3 \qquad (106)$$

(total cost).

Estimated values have to be used for the specific costs C_{magn} and C_{trit} as well as for the availability ξ and the tritium breeding ratio R.

2.3 Constraints and Optimization

In practice, several of the quantities yielded by the equations of the preceding section are subject to constraints, which stem from materials and technical limitations or are imposed by performance and design objectives. The following constraints are involved in our model:

$$g \geq g^m, \tag{107}$$

$$\Delta R \geq \Delta R^m, \tag{108}$$

$$d \geq d^m. \tag{109}$$

Here g^m, ΔR^m and d^m have the meanings outlined in Secs. 2.1 and 2.2.1.

$$\varepsilon \leq \varepsilon^m \tag{110}$$

$$\varepsilon_w \leq \varepsilon_w^m \tag{111}$$

ε^m is the maximum field ripple, while ε_w^m gives the maximum allowable strain in the superconducting windings (see eqs. (18) and (53)). The same value is used for the layout of TF coils and a superconducting OH transformer.

The neutron dose (see eq. (27)) behind the shielding is limited by the condition

$$\dot{\gamma}_n \leq 2 \cdot 10^{21}. \tag{112}$$

This condition essentially determines the shielding thickness. The neutron dose limitation results from the cryogenic stability criterion of the conductor. The increase of the stabilizer resistivity during the lifetime of a TF coil is thus limited to a value which keeps the reduction of the conductor current below 10 %.

$$j_m \geq 1.5 \times 10^8 \qquad (113)$$

j_m is an auxiliary quantity defined by eqs. (49) and (50). Imposing the limit according to eq.(113) on j_m guarantees that critical parameter values of the superconductor and the stability criterion are not violated.

In certain cases (material tests, blanket test modules) the wall load N_n and the integral wall load W_{int} are subject to a lower limit:

$$N_n \geq N_n^m \,, \qquad (114)$$

$$W_{int} \geq W_{int}^m \,. \qquad (115)$$

The core constraint has to be treated in a different way in the normal-conducting and superconducting OH transformer cases. In the normal-conducting case it is taken into account by requiring that

$$\sigma_{OH} \leq \sigma_{OH}^m \qquad (116)$$

and

$$j_{OH} \leq j_{OH}^m \qquad (117)$$

should hold, where σ_{OH}^m is the maximum tensile stress in the OH coils and j_{OH}^m the maximum OH coil current density (see eqs. (87) and (88)). The prescription of an upper limit for j_{OH} allows for a crude treatment of the cooling problem.

For the superconducting OH transformer it is required that

$$\varepsilon_{w,OH} \leq \varepsilon_w^m \tag{118}$$

and

$$j_{m,OH} \geq 1.5 \times 10^8 \tag{119}$$

should hold. Here $\varepsilon_{w,OH}$ is the strain in the OH transformer winding (see eq. (102)). The role of eq. (119) for the OH transformer layout is analogous to that of eq. (113) for the TF coil layout.

In general, the constraints do not determine a unique solution of the basic equations. This means that generally for a wide range of input parameters a, A, Y, ... the basic equations can be solved while simultaneously meeting the constraints according to eqs. (110) to (119). (Note that the conditions given by eqs. (5), (107), (108) and (109) are automatically met through the evaluation of R_2 in Sec. 2.2). A unique solution is found by determining that combination of input parameters that minimizes the figure of merit Ø as given by eq. (106).

The optimization procedure runs as follows. The input parameters of the second group in Table I are kept fixed throughout. They are not subject to manipulations (such as q(a)) and/or have only a weak influence on relevant quantities (such as ℓ, B, δ etc.). Intervals $[a_1\ a_2]$, $[A_2\ A_2]$, ... , $[C_1\ C_2]$ are given for the input parameters of the first group. The six-dimensional space spanned by these intervals is covered with a six-dimensional equidistant grid. For each grid point the computer runs through eqs. (1) to (106) of Sec. 2.2. Whenever the resulting Ø value is larger than the stored one or if any of the constraints is violated, the results for this point are

ignored and the computation is repeated for the next point. In the opposite case the results for this grid point, including $\emptyset$ and the values for a, A, ..., C, are stored.

After the computation has been performed for all grid points, the stored one is that yielding a solution with minimum $\emptyset$. Around this point a new grid of smaller size is defined and the whole procedure is repeated. This procedure is iterated to the desired accuracy.

Owing to its discrete nature the coil number N requires a distinct treatment. First the optimum solutions are determined as described above, N being kept fixed. After repetition for all N with $N_1 \leq 2N \leq N_2$, where N_1 and N_2 are input parameters, the one that yields a minimum value for $\emptyset$ is selected and taken as final solution.

An additional comment has to be made about the determination of the quantity X in eqs. (84) and (90). When the program enters the OH transformer calculation for a certain grid point, both R_{OH}^m and the OH flux swing are given. The only remaining freedom in the OH transformer layout lies in the choice of R_{OH} or, equivalently, X. Whether the constraints according to eqs. (116) and (111) or (118) and (119) are met depends, apart from R_{OH}^m and the OH flux, on the proper choice of X. Therefore for each grid point the OH transformer constraints are verified in the whole range $0.01 \leq X \leq 1$. If both constraints are met for a certain value of X, the program proceeds with this value. If no X value is found such that the constraints are met, the core constraint is considered to be violated for the respective grid point and the computation proceeds to the next grid point.

If the input intervals $[a_1\ a_2]$, $[A_1\ A_2]$, ... , $[C_1\ C_2]$ are appropriately chosen, the resulting values for a, A, ..., C, N should not coincide with either of the boundaries. This, however, may be impossible if the range of some variable is limited by physical or technical constraints or if the minimum is always taken at the boundary of the respective quantity. Whether this occurs or not depends on, apart from the variable, the whole set of constraints. The ignition factor C, for instance, thus generally takes its minimum value C_1, except when N_n^m is sufficiently high. Similarly, one finds Y = 0, except when the ripple constraint requires higher R_2 values than the constraints given by eqs. (5), (107), (108) and (109). For a specific case under consideration it is, however, easy to decide what situation prevails. Frequently, quantities such as C and Y can thus be explicitly prescribed. The resulting reduction of the grid dimension considerably reduces the computation time. The preceding discussion explains why Y was used as grid variable in Sec. 2.2.1 instead of R_2. It further shows that there is basically no difference between the constraints discussed so far and the upper and lower grid values.

The number of grid points, the number of subsequent grids and the reduction factor for the grid size can be prescribed as input parameters.

The number of grid points, and hence the computation time, strongly increases with the grid dimension. A number of six variables practically constitutes an upper limit. A typical run with maximum grid dimension, yielding an accuracy of a few p.p.th., then requires less than 60s on a CRAY I.

3. ILLUSTRATIVE EXAMPLE

As a check and for illustration we apply the SUPERCOIL model to the present INTOR layout [12] by taking the INTOR data as input for the code. The input data are listed in Table II.

The ignition margin was evaluated for the present INTOR layout on the basis of the model involved in SUPERCOIL (see eq. (20)). The resulting value was then taken as input.

The reference neutron wall load was determined by an analogous procedure resulting in a value of 1.82 MW/m^2 instead of the INTOR value of 1.3 MW/m^2. The discrepancy is partly due to a more optimistic estimation of the useful beta according to eq. (19) and partly due to a more optimistic estimation of the fusion power density according to eq. (21). To rescale to INTOR assumptions, quantities which are proportional to p_f have to be divided by 1.4.

In Table III the main output data as given by SUPERCOIL are listed. Obviously, the INTOR data are well reproduced. Further applications of SUPERCOIL to INTOR-like systems are reported in Ref. 13.

References

1. K. Borrass, M. Söll, Normal-conducting Steady-State Toroidal Magnet Systems for Ignited Tokamaks, Journal of Fusion Energy, Vol. 2, No. 1 (1982)

2. K. Borrass, M. Söll, Normal-conducting Steady-State Toroidal Magnet Systems for Large Tokamaks, Proceedings of the 9th Symp. on Eng. Probl. of Fusion Research (Chicago, 1981), pp. 150-153

3. M. Söll, An analytical approach for calculating the magnetic field ripple of toroidal D-coil magnet systems. Interner Bericht No. 24, Max-Planck-Institut für Plasmaphysik, Garching, Projekt Systemstudien (June 1979)

4. R.W. Moses, W.C. Young, Analytic expressions for magnetic forces on sectored toroidal coils, Proc. 6th Symp. on Eng. Probl. of Fusion Research (San Diego, 1975), p. 917 (1976)

5. B.J. Maddock, G.B. James, Protection and stabilization of large superconducting coils, Proc. IEE 115 (1968) 543

6. M. Söll, Maximum attainable toroidal magnetic fields for tokamaks, IEEE Tr. on Magnetics, MAG-15/1 (1979) 752

7. J. File, R.G. Mills, G.V. Scheffield, Large superconducting magnet designs for fusion reactors, MATT-848, Plasma Physics Laboratory, Princeton University (1971)

8. J. Raeder, Some analytical results for toroidal magnetic field coils with elongated minor cross-sections, Report IPP 4/141, Max-Planck-Institut für Plasmaphysik, Garching (September 1976)

9. F.R. Fickett, A review of resistive mechanisms in aluminium, Cryogenics 11 (1971) 349

10. C.H. Dustmann et al., Supraleitungstechnologie für Fusionsmagnete, Kernforschungszentrum Karlsruhe, Report KFK 2359 (1976)

11. R. J. Roark, W.C. Young, Formulas for stress and strain, 5th edition McGraw-Hill Book Company (1975)

12. INTOR, International Tokamak Reactor, Phase One, STI/PUP/619 ISBN 92-0-131082-X, IAEA, Vienna (1982)

13. K. Borrass, Sensitivity of the present INTOR layout to variations of some performance objectives, Max-Planck-Institut für Plasmaphysik Report IPP 2/257 (May 1982)

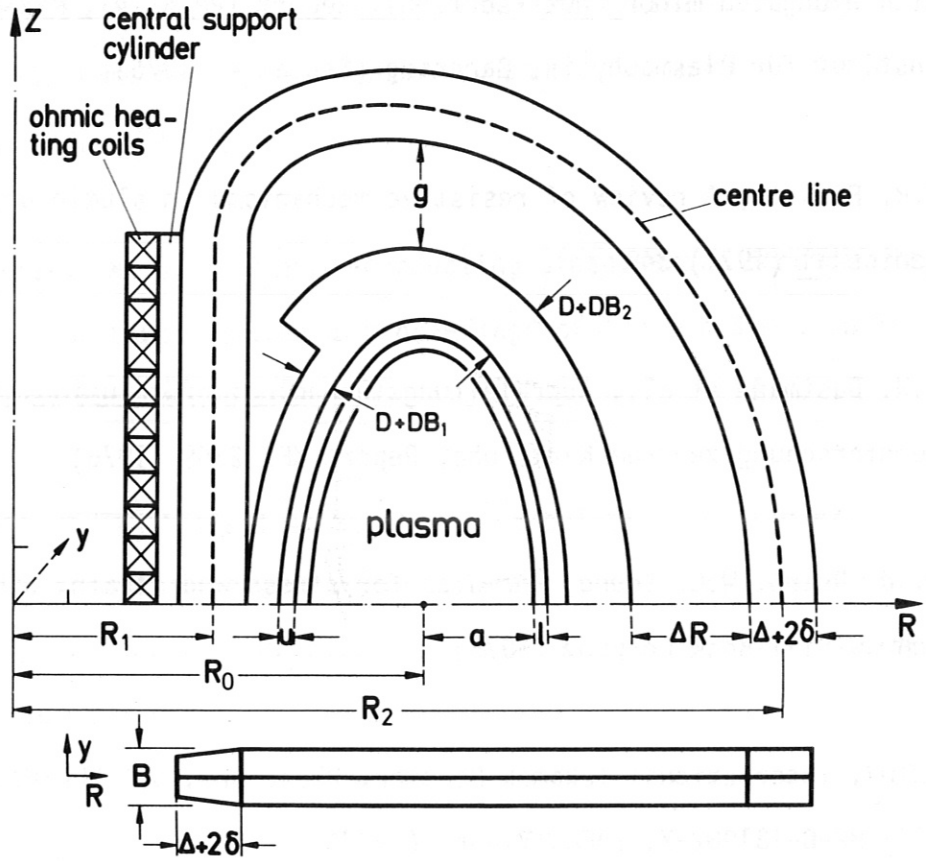

Fig. 1

Geometrical arrangement of main components

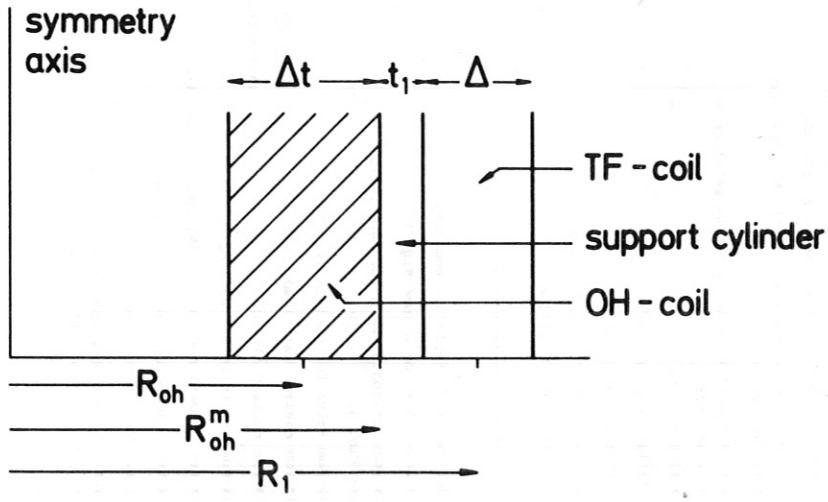

Fig. 2

Geometrical arrangement of OH transformer and central support cylinder for a superconducting OH transformer. In the normal-conducting case the thermal insulation has to be included.

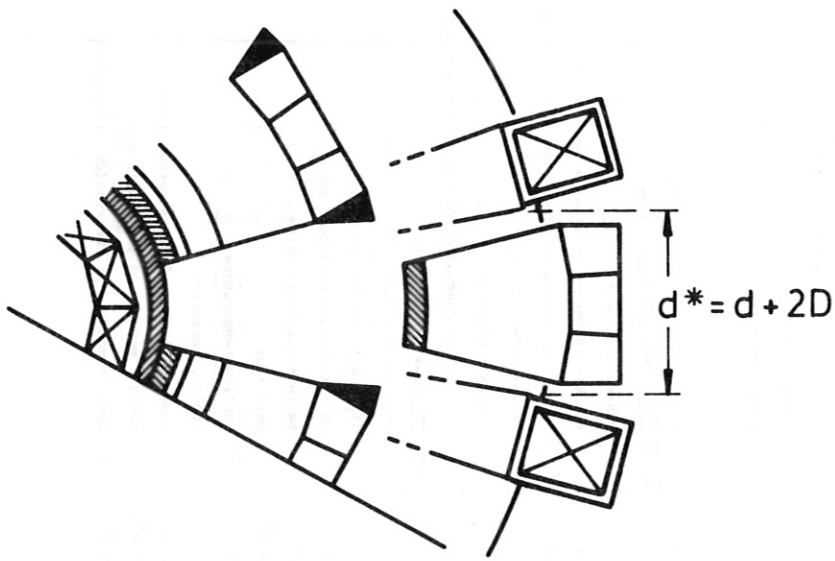

Fig. 3

Illustration of the maintenance condition

Table I

Set of input parameters required for solution of the basic equations

a	(m)	plasma minor radius	
A		aspect ratio	
Y	(m)	auxiliary quantity (see section 2.2.1 and 2.3)	
D	(m)	shielding thickness	
Δ	(m)	coil thickness (without thermal insulation and casing thickness)	GROUP I selfconsistently determined
C		ignition margin	
N		coil number	
δ	(m)	thermal insulation thickness	
ℓ	(m)	scrape-off layer thickness	
u	(m)	vessel thickness	
DB_1	(m)	blanket thickness at inner side (without shielding)	
DB_2	(m)	blanket thickness at outer side (without shielding)	
q(a)		plasma safety factor	
s		plasma elongation	
d_1, d_2	(m)	calibration constants for the maintenance condition	
λ		OH field swing factor	
f		poloidal flux enhancement factor	
η_1		filling factor for the winding	GROUP II fixed
I_{OH}	(A)	OH transformer conductor current	
V_m	(V)	maximum discharge voltage	
q	(W/m^2)	heat flux	
T	(K)	cooling temperature	
H_g		cooling parameter	
E_{sc}	(N/m^2)	Young's modulus of the superconductor	
E_{st}	(N/m^2)	Young's modulus of the stabilizer	
E_r	(N/m^2)	Young's modulus of the reinforcing material	
E_{cy}	(N/m^2)	Young's modulus of the support cylinder	
B	(m)	thickness of coil casing	
d_f	(m)	diameter of the superconducting filament	
ℓ_p	(m)	twist length of the filaments	
$\Delta B_\perp$	(T)	mean amplitude of the perpendicular poloidal magnetic induction at the toroidal winding	
$\dot{B}_\perp$	(T/sec)	rate of magnetic field variation perpendicular to the conductor	
$\dot{B}_{\|\|}$	(T/sec)	rate of magnetic field variation parallel to the conductor	
τ_{tot}	(s)	total burn time	
ξ		lifetime duty factor	
R		tritium breeding ratio	
C_{magn}	(DM/MJ)	specific cost of stored energy	
C_{trit}	(DM/g)	specific cost of tritium	
ϵ^m	(%)	maximum field ripple (at boundary)	
g^m	(m)	minimum value for g (see Fig. 1)	
d^m	(m)	minimum horizontal bore for beam parts (see Fig. 3)	
ΔR^m	(m)	minimum value for ΔR (see Fig. 1)	
N_n^m	(MW/m^2)	minimum neutron wall load	GROUP III constraints
W_{int}^m	(MW Y/m^2)	minimum neutron fluence	
ϵ_w^m		maximum strain in the winding	
σ_{cy}^m	(N/m^2)	maximum allowable stress in the support cylinder	
σ_{OH}^m	(N/m^2)	maximum tensile stress in the OH coils	
j_{OH}^m	(A/m^2)	maximum OH current density	
$j_m^{I,II}$	(A/m^2)	minimum allowable current densities in NbTi (I) and NB_3Sn (II) respectively	

a_2	(m)	1.7
A_2		5.0
Y_2	(m)	1.0
D_2	(m)	1.0
Δ_2	(m)	1.1
C_2		5.0
N_2		12
a_1	(m)	1.0
A_1		3.2
Y_1	(m)	0.0
D_1	(m)	0.4
Δ_1	(m)	0.45
C_1		4.0
N_1		12
ε^m	(%)	0.60
g^m	(m)	0.0
d^m	(m)	0.7
ΔR^m	(m)	0.0
N_n^m	(MW/m^2)	1.82
W_{int}^m	($MW\,Y/m^2$)	6.5
ε_w^m		1.0×10^{-3}
σ_{cy}^m	(N/m^2)	3.0×10^8
σ_{OH}^m	(N/m^2)	---
j_{OH}^m	(A/m^2)	---
δ	(m)	0.15
ℓ	(m)	0.2
u	(m)	0.15
DB_1	(m)	0.0
DB_2	(m)	0.78

q(a)		2.1
s		1.6
d_1	(m)	0.5
d_2	(m)	0.2
λ		2.0
f		1.5
η_1		0.85
I_{OH}	(A)	2.0×10^4
V_m	(V)	2.0×10^5
$\dot{q}$	(W/m^2)	3.0×10^3
T	(K)	4.5
H_g		4.0
E_{sc}	(N/m^2)	6.0×10^{11}
E_{st}	(N/m^2)	1.0×10^{11}
E_r	(N/m^2)	2.0×10^{11}
E_{cy}	(N/m^2)	2.0×10^{11}
B	(m)	0.05
d_f	(m)	2.0×10^{-5}
ℓ_p	(m)	0.15
$\Delta B_\perp$	(T)	0.5
$\dot{B}_\perp$	(T/s)	0.1
$\dot{B}_{\|\|}$	(T/s)	0.1
τ_{tot}	(s)	---
ξ		0.3
R		0.6
C_{magn}	(DM/MJ)	1.0×10^5
C_{trit}	(DM/g)	7.0×10^3

Table II

Complete list of input parameters for an INTOR-like system

Geometry

a	(m)	1.22	plasma minor radius
A		4.27	aspect ratio
Y	(m)	6.25×10^{-2}	see section 2.2.1
D	(m)	0.769	shielding thickness
Δ	(m)	0.877	coil thickness (without thermal insulation)
R_1	(m)	2.28	inner coil radius
R_2	(m)	12.0	outer coil radius
d	(m)	2.74	see Fig. 3

Plasma

B_t^o	(T)	5.39	field at axis
$\bar{\beta}_t$		4.50×10^{-2}	toroidal beta (volume average, useful part)
C		4.06	ignition margin (not normalized)
P_α	(MW)	166	α-power
N_n	(MW/m^2)	1.82	neutron wall load
W_{int}	($MW\,Y/m^2$)	6.49	neutron fluence
I_p	(H)	6.52×10^6	plasma current
V_s	(V)	115	OH flux swing

Toroidal Field System

B_m	(T)	10.3	field at coil
K		8.35×10^{-1}	coil parameter
σ	(N/m^2)	1.61×10^8	average mechanical stress in the winding
E_m	(GJ)	49.4	stored magnetic energy (TF system)
j_c	(A/m^2)	4.26×10^9	critical current density in the superconductor (Nb_3Sn at liquid helium temperature)
j_w	(A/m^2)	1.17×10^7	average current density in the winding
α		1.20×10^2	average ratio of the cross section area between stabilizer and superconductor (TF coil)
β		1.89×10^2	average ratio of the cross section area between reinforcing material and superconductor (TF coil)
ε_w		1.00×10^{-3}	strain in the winding

OH Transformer

t_1	(m)	2.77×10^{-1}	thickness of the support cylinder
R_{OH}	(m)	1.41	OH transformer radius
B_{OH}	(T)	9.14	OH field
$\varepsilon_{W,OH}$		9.97×10^{-3}	OH transformer winding strain

Table III

Selective list of output data for the system defined by the input data of Table II